Journal of Visualized Experiments

A Model of Reverse Vascular Remodeling in Pulmonary Hypertension Due to Left Heart Disease by Aortic Debanding in Rats

--Manuscript Draft--

Article Type:	Invited Methods Article - JoVE Produced Video
Manuscript Number:	JoVE63502R2
Full Title:	A Model of Reverse Vascular Remodeling in Pulmonary Hypertension Due to Left Heart Disease by Aortic Debanding in Rats
Corresponding Author:	Mariya Kucherenko German Heart Institute: Deutsches Herzzentrum Berlin Berlin, Please Select GERMANY
Corresponding Author's Institution:	German Heart Institute: Deutsches Herzzentrum Berlin
Corresponding Author E-Mail:	mariya.kucherenko@charite.de
Order of Authors:	Mariya M. Kucherenko
	Pengchao Sang
	Juquan Yao
	Qiuhua Li
	Szandor Simmons
	Wolfgang M. Kuebler
	Christoph Knosalla
Additional Information:	
Question	**Response**
Please specify the section of the submitted manuscript.	Medicine
Please indicate whether this article will be Standard Access or Open Access.	Standard Access ($1400)
Please indicate the **city, state/province, and country** where this article will be **filmed**. Please do not use abbreviations.	Berlin/Germany
Please confirm that you have read and agree to the terms and conditions of the author license agreement that applies below:	I agree to the Author License Agreement
Please confirm that you have read and agree to the terms and conditions of the video release that applies below:	I agree to the Video Release
Please provide any comments to the journal here.	

TITLE:

A Model of Reverse Vascular Remodeling in Pulmonary Hypertension Due to Left Heart Disease by Aortic Debanding in Rats

AUTHORS AND AFFILIATIONS:

Pengchao Sang[1,2,3], Mariya M. Kucherenko[1,2,3]*, Juquan Yao[2], Qiuhua Li[2], Szandor Simmons[2,3], Wolfgang M. Kuebler[2,3#], Christoph Knosalla[1,3,4#]

[1]Department of Cardiothoracic and Vascular Surgery, German Heart Center Berlin (DHZB), Augustenburger Platz 1, 13353 Berlin

[2]Institute of Physiology, Charité – Universitätsmedizin Berlin, corporate member of Freie Universität Berlin, Humboldt-Universität zu Berlin, and Berlin Institute of Health, Charitéplatz 1, 10117 Berlin

[3]DZHK (German Centre for Cardiovascular Research), Partner Site Berlin

[4]Charité – Universitätsmedizin Berlin, corporate member of Freie Universität Berlin, Humboldt-Universität zu Berlin, and Berlin Institute of Health, Charitéplatz 1, 10117 Berlin

Email addresses of the authors:

Pengchao Sang (peng-chao.sang@charite.de)
Mariya M. Kucherenko (mariya.kucherenko@charite.de)
Juquan Yao (juquan.yao@charite.de)
Qiuhua Li (qiuhua.li@charite.de)
Szandor Simmons (szandor.simmons@charite.de)
Wolfgang M. Kuebler (wolfgang.kuebler@charite.de)
Christoph Knosalla (knosalla@dhzb.de)

*Email address of the corresponding author:

Mariya M. Kucherenko (mariya.kucherenko@charite.de)

[#]These authors contributed equally

SUMMARY:

The present protocol describes a surgical procedure to remove ascending-aortic banding in a rat model of pulmonary hypertension due to left heart disease. This technique studies endogenous mechanisms of reverse remodeling in the pulmonary circulation and the right heart, thus informing strategies to reverse pulmonary hypertension and/or right ventricular dysfunction.

ABSTRACT:

Pulmonary hypertension due to left heart disease (PH-LHD) is the most common form of PH, yet its pathophysiology is poorly characterized than pulmonary arterial hypertension (PAH). As a result, approved therapeutic interventions for the treatment or prevention of PH-LHD are missing. Medications used to treat PH in PAH patients are not recommended for treatment of PH-LHD, as reduced pulmonary vascular resistance (PVR) and increased pulmonary blood flow in the presence of increased left-sided filling pressures may cause left heart decompensation and

pulmonary edema. New strategies need to be developed to reverse PH in LHD patients. In contrast to PAH, PH-LHD develops due to increased mechanical load caused by congestion of blood into the lung circulation during left heart failure. Clinically, mechanical unloading of the left ventricle (LV) by aortic valve replacement in aortic stenosis patients or by implantation of LV assist devices in end-stage heart failure patients normalizes not only pulmonary arterial and right ventricular (RV) pressures but also PVR, thus providing indirect evidence for reverse remodeling in the pulmonary vasculature. Using an established rat model of PH-LHD due to left heart failure triggered by pressure overload with subsequent development of PH, a model is developed to study the molecular and cellular mechanisms of this physiological reverse remodeling process. Specifically, an aortic debanding surgery was performed, which resulted in reverse remodeling of the LV myocardium and its unloading. In parallel, complete normalization of RV systolic pressure and significant but incomplete reversal of RV hypertrophy was detectable. This model may present a valuable tool to study the mechanisms of physiological reverse remodeling in the pulmonary circulation and the RV, aiming to develop therapeutic strategies for treating PH-LHD and other forms of PH.

INTRODUCTION:

Heart failure is the leading cause of death in developed countries and is expected to increase by 25% over the next decade. Pulmonary hypertension (PH) – a pathological increase of blood pressure in the pulmonary circulation – affects approximately 70% of patients with end-stage heart failure; the World Health Organization classifies PH as pulmonary hypertension due to left heart disease (PH-LHD)[1]. PH-LHD is initiated by impaired systolic and/or diastolic left ventricular (LV) function that results in elevated filling pressure and passive congestion of blood into the pulmonary circulation[2]. Albeit initially reversible, PH-LHD gradually becomes fixed due to active pulmonary vascular remodeling in all compartments of the pulmonary circulation, i.e., arteries, capillaries, and veins[3,4]. Both reversible and fixed PH increase RV afterload, initially driving adaptative myocardial hypertrophy but ultimately causing RV dilatation, hypokinesis, fibrosis, and decompensation that progressively lead to RV failure[1,2,5,6]. As such, PH accelerates disease progression in heart failure patients and increases mortality, particularly in patients undergoing surgical treatment by implantation of left ventricular assist devices (LVAD) and/or heart transplantation[7-9]. Currently, no curative therapies exist that could reverse the process of pulmonary vascular remodeling, so fundamental mechanistic research in appropriate model systems is needed.

Importantly, clinical studies show that PH-LHD as a frequent complication in patients with aortic stenosis can improve rapidly in the early post-operative period following aortic valve replacement[10]. Analogously, high (>3 Wood Units) pre-operative pulmonary vascular resistance (PVR) that was, however, reversible on nitroprusside was sustainably normalized after heart transplantation in a 5-year follow-up study[11]. Similarly, an adequate reduction of both reversible and fixed PVR and improvement of RV function in LHD patients could be realized within several months by unloading the left ventricle using implantable pulsatile and non-pulsatile ventricular assist devices[12-14]. Currently, the cellular and molecular mechanisms that drive reverse remodeling in the pulmonary circulation and RV myocardium are unclear. Yet, their understanding may provide important insight into physiological pathways that may be

therapeutically exploited to reverse lung vascular and RV remodeling in PH-LHD and other forms of PH.

A suitable preclinical model that adequately replicates the pathophysiological and molecular features of PH-LHD can be used for translational studies in pressure overload-induced congestive heart failure due to surgical aortic banding (AoB) in rats[4,15,16]. In comparison to similar heart failure due to pressure overload in the murine model of transverse aortic constriction (TAC)[17], banding of the ascending aorta above the aortic root in AoB rats does not produce hypertension in the left carotid artery as the banding site is proximal of the outflow of the left carotid artery from the aorta. As a result, AoB does not cause left-sided neuronal injury in the cortex as is characteristic for TAC[18], and which may affect the study outcome. Compared to other rodent models of surgically induced PH-LHD, rat models in general, and AoB in particular, prove to be more robust, reproducible and replicate the remodeling of the pulmonary circulation characteristic for PH-LHD patients. At the same time, perioperative lethality is low[19]. Increased LV pressures and LV dysfunction in AoB rats induce PH-LHD development, resulting in elevated right ventricular pressures and right ventricular (RV) remodeling. As such, the AoB rat model has proven extremely useful in a series of previous studies by independent groups, including ourselves, to identify pathomechanisms of pulmonary vascular remodeling and test potential treatment strategies for PH-LHD[4,15,20-25].

In the present study, the AoB rat model was utilized to establish a surgical procedure of aortic debanding to study mechanisms of reverse remodeling in the pulmonary vasculature and the RV. Previously, myocardial reverse remodeling models such as aortic debanding in mice[26] and rats[27] have been developed to investigate the cellular and molecular mechanisms regulating the regression of left ventricular hypertrophy and test potential therapeutic options to promote myocardial recovery. Moreover, a limited number of earlier studies have explored the effects of aortic debanding on PH-LHD in rats and showed that aortic debanding might reverse medial hypertrophy in pulmonary arterioles, normalize the expression of pre-pro-endothelin 1 and improve pulmonary hemodynamics[27,28], providing evidence for the reversibility of PH in rats with heart failure. Here, the technical procedures of the debanding surgery are optimized and standardized, e.g., by applying a tracheotomy instead of endotracheal intubation or by using titanium clips of a defined inner diameter for aortic banding instead of polypropylene sutures with a blunt needle[26,27], thus providing for better control of the surgical procedures, increased reproducibility of the model and an improved survival rate.

From a scientific perspective, the significance of the PH-LHD debanding model does not solely lie in demonstrating the reversibility of the cardiovascular and pulmonary phenotype in heart failure, but more importantly, in the identification of molecular drivers that trigger and/or sustain reverse remodeling in pulmonary arteries as promising candidates for future therapeutic targeting.

PROTOCOL:

All procedures were performed following the "Guide for the Care and Use of Laboratory Animals" (Institute of Laboratory Animal Resources, 7th edition 1996) and approved by the local

governmental animal care and use committee of the German State Office for Health and Social Affairs (Landesamt für Gesundheit und Soziales (LaGeSO), Berlin; protocol no. G0030/18). First, congestive heart failure was surgically induced in juvenile Sprague-Dawley rats ~100 g body weight (bw) (see **Table of Materials**) by placing a titanium clip with a 0.8 mm inner diameter on the ascending aorta (aortic banding, AoB) as described previously[29,30]. At week 3 after AoB (**Figure 1**), debanding (Deb) surgery was performed to remove the clip from the aorta. The surgical procedures and validation of PH reversal in AoB rats performed are schematically depicted in **Figure 1**.

1. Surgical preparations

1.1. Prepare surgical instruments (**Figure 2**) and soak them in 70% ethanol for 30 min.

1.2. Inject carprofen (5 mg/kg bw) (see **Table of Materials**) intraperitoneally (i.p.) for analgesia 30 min prior to surgery.

1.3. Anesthetize rat by i.p. injection of ketamine (87 mg/kg bw) and xylazine (13 mg/kg bw).

1.4. Remove the hair from the animal's neckline and chest using an electric shaver.

1.5. Apply a drop of eye ointment to protect the eyes during surgery.

1.6. Place the rat in a supine position on a sterilized surgical table. Carefully fix the animal's abdomen and limbs with adhesive tape.

NOTE: To maintain body temperature, place a 37 °C heating mat under the surgical table. Avoid heating of the head region to prevent drying of eyes.

1.7. Disinfect animal skin with povidone-iodine/iodophor solution. Note scars and sutures from the primary AoB surgery.

1.8. Ensure adequate depth of anesthesia by toe pinching.

NOTE: Depth of anesthesia needs to be controlled regularly during surgery.

2. Tracheotomy and mechanical ventilation

2.1. With fine scissors (**Figure 2A**), make a 7-10 mm long cervical midline incision (**Figure 3A**).

2.2. With the help of a pair of blunt forceps (**Figure 2B'**), dissect the cervical soft tissue to expose the infrahyoid muscles. Split muscles in the midline to visualize the trachea. Cut and remove the suture from the primary AoB surgery.

2.3. Make ~2 mm trachea incision between two cartilaginous rings using angled Noyes spring

scissors (**Figure 2C,3B**). Insert the tracheal cannula of outer diameter 2 mm (**Figure 2D**) into the trachea and secure it with a 4-0 silk suture (**Figure 2E,3C**).

2.4. Connect the tracheal cannula to a mechanical ventilator (see **Table of Materials**) while keeping dead space to a minimum (**Figure 3D-E**). Keep perioperative lung ventilation at a respiratory rate of 90 breaths/min at a tidal volume (Vt) of 8.5 mL/kg bw.

3. Aortic debanding

3.1. Make an ~20 mm long skin incision between the second and third ribs using fine scissors (**Figure 3F**).

3.2. With the help of smaller surgical scissors (**Figure 2F**), carefully spread muscles and cut them layer by layer (**Figure 3G**). Make a 10 mm lateral incision along the intercostal space between the second and third rib.

NOTE: The midsternal line needs to be carefully approached to avoid bleeding.

3.3. Use a rib spreader (**Figure 2G**) to expand the intercostal space between the second and third rib to create a surgical window (**Figure 3H**).

3.4. With the help of blunt forceps (**Figure 2B,B'**), carefully separate the thymus from the heart and conduit arteries to visualize the aorta with the clip (**Figure 4A**).

3.5. Hold the clip with the help of the forceps and carefully remove the connective tissue around the clip to expose it.

NOTE: Avoid holding or lifting the aorta with the forceps, as it may injure the aorta resulting in bleeding and a lethal outcome.

3.6. With the help of a needle holder (**Figure 2H**), open the clip (**Figure 4B**) and remove it from the thoracic cavity.

3.7. Before closing the chest, open up lung atelectasis, ensure adequate lung recruitment without overdistension, continue mechanical ventilation with a Vt of 9.5 mL/kg bw for another 10 min, and return to a Vt of 8.5 mL/kg bw.

3.8. Close the deep muscles by a simple interrupted suture using 4-0 silk. Then connect the upper muscles and the skin with a simple continuous suture (**Figure 5A,B**).

4. Tracheal extubation

4.1. Disconnect the tracheal cannula from the ventilation machine. Attentively observe the rat until spontaneous breathing is re-established. If the animal fails to breathe spontaneously

upon disconnection, reconnect the ventilator and continue ventilating for an additional 5 min. Then repeat the procedure.

4.2. After spontaneous breathing is re-established, remove the cannula from the trachea and clean the liquid around the trachea with sponge points (**Figure 2I**) (see **Table of Materials**).

4.3. Close the trachea with a simple suture using 6-0 prolene (**Figure 2E'** and **Figure 5C**). Then close infrahyoid muscles in a simple interrupted suture using 4-0 silk (**Figure 5D**), and connect the skin in a simple continuous suture (**Figure 5E**). Clean and disinfect the muscles and the skin during the process with povidone-iodine/iodophor solution.

5. Post-operative care

5.1. After completing the surgical procedure, carefully move the animal to a recovery cage with supplemental oxygen and an infra-red lamp to keep animals warm and sufficiently oxygenated during the recovery phase. Place the oxygen mask close to the rat's snout. Only keep one animal per recovery cage at any time.

5.2. After the animal wakes up, carefully move it to a regular cage supplied with water and food. For the next 12 h, control the health status of the operated animal in 2 h intervals.

5.3. After completing the surgical procedure, apply analgesia daily by i.p. injection of carprofen (5 mg/kg bw) for one week.

5.4. To avoid bacterial infection, administer amoxicillin (500 mg/L) in the drinking water for one week postoperatively.

REPRESENTATIVE RESULTS:

First, successful aortic debanding was confirmed by transthoracic echocardiography performed before and after the debanding procedure in AoB animals (**Figure 6**). To this end, the aortic arch was assessed in PLAX B-mode view. The position of the clip on the ascending aorta in AoB animals and its absence after the Deb surgery was visualized (**Figure 6A,B**). Next, aortic blood flow was evaluated by pulsed-wave Doppler imaging (**Figure 6C-F**). Peak blood flow velocity in AoB animals measured before and after the clip was 733.24 ± 17.39 mm/s and 5215.08 ± 48.05 mm/s (n = 8 animals), respectively (**Figure 6C,E**), demonstrating a steep gradient across the AoB site. After clip removal, peak blood flow velocity was 1093.79 ± 28.97 mm/s and 2578.73 ± 42.27 mm/s, respectively, at corresponding aortic locations, showing a marked attenuation of the gradient in line with functional debanding (**Figure 6D,F**). To probe for reversal of left heart failure by aortic debanding, the expression levels of brain natriuretic peptide (BNP) were accessed, a clinical routine parameter for assessing heart disease[31], in the LV myocardium. At weeks 3 and 5 after aortic banding, AoB animals showed a significantly increased production of BNP in comparison to sham-operated controls. In contrast, Deb rats at week 5 expressed BNP at levels comparable to sham animals, indicating the reversal of LV failure by aortic debanding (**Figure 7A-C**). In parallel, evaluation of LV function by transthoracic echocardiography revealed an increased LV

ejection fraction and LV volume in Deb animals compared to AoB rats (**Figure 7D-E**). While LV ejection fraction in Deb animals was comparable to sham rats, LV volume in Deb rats failed to fully normalize to values seen in the sham group, indicating that reversal of LV function is incomplete.

To probe whether Deb animals may serve as a preclinical model to study reverse pulmonary vascular and right ventricular (RV) remodeling in PH-LHD, left ventricular systolic pressure (LVSP), and right ventricular systolic pressure (RVSP) was assessed using a microtip Millar catheter. In brief, rats were again anesthetized with ketamine (87 mg/kg bw) and xylazine (13 mg/kg bw), tracheotomized, and ventilated as described above. Cardiac catheterization was performed after median thoracotomy[32] through the apex of (first) the left and (second) the right ventricle, respectively, as direct catheterization of the left ventricle *via* the vascular route is prevented by the aortic band in AoB animals. Following euthanasia by an overdose of ketamine/xylazine, the heart was excised, and ventricular hypertrophy was assessed as the weight of the left ventricle including septum (LV+S) or the right ventricle (RV) normalized to body weight (BW). In accordance with AoB rats as an established model for PH-LHD, AoB animals showed a significantly increased LVSP and RVSP and LV and RV hypertrophy compared to sham-operated animals at 3 weeks after post-surgery (**Figure 8A-F**). Debanding (Deb) surgery performed at week 3 after AoB resulted in a significant reduction of both LVSP and LV hypertrophy in comparison to AoB animals without Deb at week 3 and week 5 post-AoB, demonstrating that normalization of LV hemodynamics following clip removal from the aorta reversed LV remodeling (**Figure 8C,D**). Compared to AoB rats at week 3 and week 5, Deb animals also showed a significant reduction in RVSP and RV/BW, demonstrating successful reversal of PH-LHD (**Figure 8E,F**). Notably, RVSP in Deb rats was comparable to values measured in sham animals, indicating a complete normalization of RV hemodynamics. In contrast, RV hypertrophy in Deb animals was only partially reversed with RV/BW, remaining significantly increased compared to sham controls (**Figure 8E,F**).

FIGURE LEGENDS:

Figure 1: Schematic representation of the surgical procedures and validation of PH reversal in AoB rats. The schematic depicts the different experimental groups used in the present study to test whether debanding surgery reverses PH-LHD. Sham, sham-operated controls; AoB, aortic banding; Deb, debanding. Triangles mark the time point of surgical interventions: primary operation (sham or AoB; red) at week 0 and secondary operation (Deb; green) at week 3. Circles mark the end-point analyses at which PH-LHD was assessed by LV and RV pressures and hypertrophy measurements, respectively.

Figure 2: Surgical instruments. (**A**) Fine scissors Tungsten carbide. (**B)** Moria Iris forceps and (**B'**) Serrated Graefe forceps. The forceps' tips are shown enlarged. (**C**) Noyes spring scissors. (**D**) Tracheal cannula. (**E**, **E'**) 4-0 and 6-0 sutures, respectively. (**F**) Fine scissors Tungsten carbide. (**G**) Rib spreader. (**H**) Mathieu needle holder. (**I**) Sponge points tissue.

Figure 3: Tracheotomy and thoracotomy. Images illustrate the surgical steps for the tracheotomy. (**A**) Cervical midline incision. (**B**) Incision of the trachea between two cartilaginous

rings. (**C**) Tracheal cannula inserted into the trachea and secured with a suture. (**D**) The tracheal cannula is connected to a mechanical ventilator. (**E**) Images illustrate the surgical steps for the thoracotomy. (**F**) Skin incision between the second and third ribs. (**G**) Cutting of muscles. (**H**) Creation of a thoracic surgical window by spreading the second and the third ribs.

Figure 4: Visualization of the aortic-constricting clip *in vivo* and *ex vivo.* (**A**) The image shows the thoracic cavity of an AoB rat with a titanium clip placed on the ascending aorta. (**B**) The image shows closed and opened clip *ex vivo*. Asterisk marks the part of the clip that the needle holder compresses *in vivo* to open the clip.

Figure 5: Wound closure. Images illustrate the closing of the upper thoracic muscles (**A**) and the skin (**B**) with a simple continuous suture. The trachea (**C**) and the infrahyoid muscles (**D**) are closed by a simple suture and the skin on the neck (**E**) by a simple continuous suture.

Figure 6: Aortic blood flow prior to and after debanding surgery. (**A-B**) Visualization of the ascending aorta in a rat with aortic banding (AoB, left) and a rat after debanding surgery (Deb, right) by transthoracic echocardiography. The arrow shows the titanium clip on the aorta in (**A**) absent in (**B**). (**C,D**) Pulsed-wave Doppler echocardiographic images show blood flow before the clip in an AoB rat (**C**) and blood flow in the corresponding aortic segment in a Deb rat (**D**) taken one day prior and one day after the aortic debanding surgery, respectively. (**E,F**) Analogously, images show blood flow in the aortic segment after the clip in an AoB rat (**E**) and in the corresponding aortic segment in a Deb rat (**F**) taken one day prior and one day after the aortic debanding surgery, respectively. Turquois vertical lines illustrate measurements of peak aortic flow velocity.

Figure 7: Normalization of left ventricular function by aortic debanding. (**A**) Representative Western blots show protein levels of BNP and with GAPDH as loading control in left ventricles (LV) of AoB rats at week 3 after aortic banding (n = 5) and in corresponding sham controls (n = 5). (**B**) Representative Western blots show BNP and GAPDH in left ventricles (LV) of AoB rats at week 5 after aortic banding (n = 4), in Deb rats at week 5 (n = 5), and in sham controls at the corresponding time after primary surgery (n = 4). (**C)** Box and whisker plots show quantification of BNP expression normalized to GAPDH and sham control at the corresponding time after primary surgery. Boxes show median, 25, and 75 percentiles, respectively; whiskers indicate the minimum and maximum values. For statistical analyses, Student's t-test[33] was used. **p*-value < 0.05. (**D**) Bar graphs (mean ± standard deviation) show LV ejection fraction and volume in sham (n = 4), AoB (n = 9), and Deb (n = 7) animals at week 5 as measured by echocardiography from M- and B-mode images. (**E**) Representative M-mode echocardiographic images show changes in LV fractional shortening in sham, AoB, and Deb animals at week 5. For statistical analyses Mann–Whitney U test[33] was used. **p*-value < 0.05.

Figure 8: Ventricular hemodynamics are normalized, and cardiac hypertrophy is reversed by aortic debanding. (**A**) Representative measurements of left ventricular (LV) and right ventricular (RV) blood pressure in a rat 3 weeks after aortic banding (AoB) as compared to corresponding sham control. (**B**) Representative images show cardiac hypertrophy in an AoB rat 3 weeks after

aortic banding compared to sham control. (**C-F**) Box and whisker plots show left ventricular systolic pressure (LVSP; **C**), LV hypertrophy ([LV+S]/BW; **D**), right ventricular systolic pressure (RVSP; **E**), and RV hypertrophy (RV/BW; **F**) in sham and AoB animals at 3 and 5-weeks post-surgery, and normalized parameters (in comparison to 3- and 5-week AoB groups) in Deb rats. Boxes show median, 25, and 75 percentiles, respectively; whiskers indicate the minimum and maximum values. n = 9-12 animals were analyzed for hemodynamic measurements, and heart weight was measured in n = 7-12 rats per group. For statistical analyses Mann–Whitney U test was used. *p-value < 0.05.

DISCUSSION:

Here, a detailed surgical technique for aortic debanding in a rat AoB model is reported that can be utilized to investigate the reversibility of PH-LHD and the cellular and molecular mechanisms that drive reverse remodeling in the pulmonary vasculature and the RV. Three weeks of aortic constriction in juvenile rats results in PH-LHD evident as increased LV pressures, LV hypertrophy, and concomitantly increased RV pressures and RV hypertrophy. Aortic debanding at week 3 post-AoB was able to unload the LV and fully reverse LV hypertrophy within two weeks after Deb. In parallel, aortic debanding also caused a full normalization of RV pressures and a partial reversal of RV hypertrophy.

The present model thus mimics critical aspects of the clinical scenario where mechanical unloading of the LV by an implantable non-pulsatile LVAD with continuous flow properties has previously been found to reverse PH in patients with heart failure[34,35]. In a retrospective analysis, LVAD support was shown to reduce pulmonary artery pressure to similar degrees in heart failure patients with either reversible or fixed PH, with fixed PH defined as mean pulmonary arterial pressure >25 mm Hg, pulmonary vascular resistance >2.5 Wood Unit and a mean pressure transpulmonary gradient >12 mm Hg despite pharmacological treatment[35]. Importantly, these findings[34,35] provide indirect evidence that left ventricular unloading not only decreases passive pulmonary congestion and secondary changes in lung vascular tone but triggers reverse remodeling of the pulmonary vasculature by "physiological" mechanisms, i.e., by adaptation to altered hemodynamics. In-depth, multi-omics analyses of the cellular and molecular processes that drive reverse remodeling in the pulmonary vasculature could open up new avenues for identifying novel therapeutic options for treating PH in heart failure patients and potentially also in other forms of PH including PAH. The present model of debanding in AoB rats provides a unique possibility for such analyses as complete normalization of RVSP confirms effective reversal of PH, thus allowing for mechanistic studies to identify pathways with the ability to restore homeostatic processes in the diseased pulmonary vasculature.

With a similar rationale, the present model may further be utilized to study intra- and intercellular processes that drive reverse remodeling of the RV. RV function has recently been recognized as a significant predictor of prognosis for morbidity and mortality in cardiovascular diseases. Yet no therapies have been clinically approved to improve RV function[36]. As such, the ability to study reverse remodeling processes in the RV myocardium in an animal model provides a unique opportunity to address a significant knowledge gap and a critical medical need.

The success of the technically challenging aortic debanding procedure in AoB rats depends on surgical skills and precise perioperative strategies. Outlined in the following are critical surgical procedure steps that may cause perioperative lethality by excessive bleeding (1-5) or insufficient respiration (6) and recommendations on avoiding these complications.

(1) During a thoracotomy, the midsternal line needs to be approached carefully with scissors to avoid injury to the internal mammary artery. (2) To visualize the heart and the conduit arteries, the thymus should be mobilized and carefully relocated in the cranial direction. In the debanding surgery, the thymus tissue is often connected to the heart and arteries *via* post-operative adhesions from the original AoB surgery. These adhesions should be carefully separated with a pair of blunt forceps to avoid injury to the cardiovascular structures. (3) In the debanding surgery, the aorta with the clip is frequently embedded in connective tissue. This connective tissue must be gently dissected with blunt forceps to visualize the clip. Here, the transthoracic echocardiography performed before the surgery is a helpful preparation step, allowing to identify whether the clip is located close to the aortic root, in the middle of the ascending aorta, or close to the brachiocephalic artery. This knowledge saves precious time for clip allocation during the surgery. (4) The orientation of the clip is a critical step that must be considered carefully during the initial aortic banding surgery. To facilitate optimal assessment and rapid opening of the clip during aortic debanding, the part that needs to be compressed by the needle holder (**Figure 4B**) should be oriented ventrally. Clip reorientation during debanding surgery is feasible, although at the risk of injury to the aorta. For clip reorientation, clips need to be held by forceps while surrounding connective tissue is carefully removed, then the clip should be mobilized and turned. Holding the aorta with the forceps is to be avoided. (5) For debanding, the clip should be held by a forceps with one hand and opened with a needle holder with the other hand. The aorta need not be lifted ventrally. (6) After completing the debanding procedure, extubated PH-LHD rats are at considerable risk of respiratory failure, with animals commonly dying within 10-20 min after surgery while still under the anesthesia. Atelectasis of the left lung is the most common cause of death in this period, and prolonged mechanical ventilation before chest closure helps recruit the lung and warrant sufficient respiration after surgery.

We also suggest that compared to endotracheal intubation as performed in previous studies[26,27], tracheostomy provides better control of appropriate ventilation during surgical procedures, which is specifically relevant during aortic debanding. This notion is based on the following rationale: (1) Tracheostomy, routinely performed in our lab for perioperative lung ventilation, is a straightforward and safe technique with no perioperative or post-operative complications. (2) Tracheostomy eliminates the risk of esophageal intubation or tracheal injury; it enables precise positioning and fixation of the tracheal cannula and constant visual control of the cannula during all steps of the surgical procedure. (3) At the time of aortic debanding, AoB animals are already in heart failure and are more sensitive to additional stress; as a result, the potential risks that come with endotracheal intubation may add to increased lethality. (4) Finally, when the operated animal is weaned from the ventilator but fails to develop spontaneous breathing, a tracheostomy allows for rapid reintubation and reconnection with the ventilator, thus potentially saving lives due to the ability for prolonged post-operative ventilation.

The present study reports an aortic debanding technique performed 3 weeks after initial aortic banding in rats. For studies aiming to compare reverse remodeling of the pulmonary vasculature and the RV at different PH stages, the described procedures may also be performed at later time points after aortic banding. Yet, caution is warranted as scar and connective tissue surrounding the aorta will likely become more abundant with time, further complicating the procedure and necessitating additional troubleshooting and refinement. At the same time, the basic principles of the reported protocol still apply.

ACKNOWLEDGMENTS:

This research was supported by grants of the DZHK (German Centre for Cardiovascular Research) to CK and WMK, the BMBF (German Ministry of Education and Research) to CK in the framework of VasBio, and to WMK in the framework of VasBio, SYMPATH, and PROVID, and the German Research Foundation (DFG) to WMK (SFB-TR84 A2, SFB-TR84 C9, SFB 1449 B1, SFB 1470 A4, KU1218/9-1, and KU1218/11-1).

DISCLOSURES:

The authors have no conflicts of interest to declare. All co-authors have seen and agree with the contents of the manuscript.

REFERENCES:

1. Rosenkranz, S. et al. Pulmonary hypertension due to left heart disease: Updated recommendations of the cologne consensus conference 2011. *International Journal of Cardiology.* **154** (Suppl 1), S34-44 (2011).
2. Rosenkranz, S. et al. Left ventricular heart failure and pulmonary hypertension. *European Heart Journal*. **37** (12), 942-954 (2016).
3. Fayyaz, A. U. et al. Global Pulmonary vascular remodeling in pulmonary hypertension associated with heart failure and preserved or reduced ejection fraction. *Circulation*. **137** (17), 1796-1810 (2018).
4. Hunt, J. M. et al. Pulmonary veins in the normal lung and pulmonary hypertension due to left heart disease. *The American Journal of Physiology - Lung Cellular and Molecular Physiology*. **305** (10), L725-736 (2013).
5. Bursi, F. et al. Pulmonary pressures and death in heart failure: A community study. *Journal of the American College of Cardiology*. **59** (3), 222-231 (2012).
6. Ryan, J. J. et al. Right ventricular adaptation and failure in pulmonary arterial hypertension. *Canadian Journal of Cardiology*. **31** (4), 391-406 (2015).
7. Miller, W. L., Mahoney, D. W., Enriquez-Sarano, M. Quantitative Doppler-echocardiographic imaging and clinical outcomes with left ventricular systolic dysfunction: Independent effect of pulmonary hypertension. *Circulation: Cardiovascular Imaging*. **7** (2), 330-336 (2014).
8. Kjaergaard, J. et al. Prognostic importance of pulmonary hypertension in patients with heart failure. *The American Journal of Cardiology*. **99** (8), 1146-1150 (2007).
9. Shah, R. et al. Pulmonary hypertension after heart transplantation in patients bridged with the total artificial heart. *ASAIO Journal*. **62** (1), 69-73 (2016).
10. Tracy, G. P., Proctor, M. S., Hizny, C. S. Reversibility of pulmonary artery hypertension in

aortic stenosis after aortic valve replacement. *The Annals of Thoracic Surgery*. **50** (1), 89-93 (1990).
11. Lindelow, B., Andersson, B., Waagstein, F., Bergh, C. H. High and low pulmonary vascular resistance in heart transplant candidates. A 5-year follow-up after heart transplantation shows continuous reduction in resistance and no difference in complication rate. *European Heart Journal*. **20** (2), 148-156 (1999).
12. Martin, J. et al. Implantable left ventricular assist device for treatment of pulmonary hypertension in candidates for orthotopic heart transplantation-a preliminary study. *European Journal of Cardio-Thoracic Surgery*. **25** (6), 971-977 (2004).
13. Gallagher, R. C. et al. Univentricular support results in reduction of pulmonary resistance and improved right ventricular function. *ASAIO Transactions*. **37** (3), M287-288 (1991).
14. Beyersdorf, F., Schlensak, C., Berchtold-Herz, M., Trummer, G. Regression of "fixed" pulmonary vascular resistance in heart transplant candidates after unloading with ventricular assist devices. *The Journal of Thoracic and Cardiovascular Surgery*. **140** (4), 747-749 (2010).
15. Hoffmann, J. et al. Mast cells promote lung vascular remodelling in pulmonary hypertension. *European Respiratory Journal*. **37** (6), 1400-1410 (2011).
16. Litwin, S. E. et al. Serial echocardiographic-Doppler assessment of left ventricular geometry and function in rats with pressure-overload hypertrophy. Chronic angiotensin-converting enzyme inhibition attenuates the transition to heart failure. *Circulation*. **91** (10), 2642-2654 (1995).
17. Rockman, H. A. et al. Segregation of atrial-specific and inducible expression of an atrial natriuretic factor transgene in an in vivo murine model of cardiac hypertrophy. *Proceedings of the National Academy of Sciences of the United States of America*. **88** (18), 8277-8281 (1991).
18. de Montgolfier, O. et al. High Systolic blood pressure induces cerebral microvascular endothelial dysfunction, neurovascular unit damage, and cognitive decline in mice. *Hypertension*. **73** (1), 217-228 (2019).
19. Breitling, S., Ravindran, K., Goldenberg, N. M., Kuebler, W. M. The pathophysiology of pulmonary hypertension in left heart disease. *American Journal of Physiology - Lung Cellular and Molecular Physiology*. **309** (9), L924-941 (2015).
20. Ranchoux, B. et al. Metabolic syndrome exacerbates pulmonary hypertension due to left heart disease. *Circulation Research*. **125** (4), 449-466 (2019).
21. Zhang, H., Huang, W., Liu, H., Zheng, Y., Liao, L. Mechanical stretching of pulmonary vein stimulates matrix metalloproteinase-9 and transforming growth factor-beta1 through stretch-activated channel/MAPK pathways in pulmonary hypertension due to left heart disease model rats. *PLoS One*. **15**, e0235824 (2020).
22. Yin, J. et al. Sildenafil preserves lung endothelial function and prevents pulmonary vascular remodeling in a rat model of diastolic heart failure. *Circulation: Heart Failure*. **4** (2), 198-206 (2011).
23. Yin, N. et al. Inhaled nitric oxide versus aerosolized iloprost for the treatment of pulmonary hypertension with left heart disease. *Critical Care Medicine*. **37** (3), 980-986 (2009).
24. Breitling, S. et al. The mast cell-B cell axis in lung vascular remodeling and pulmonary hypertension. *American Journal of Physiology - Lung Cellular and Molecular Physiology*. **312** (5), L710-L721 (2017).
25. Kerem, A. et al. Lung endothelial dysfunction in congestive heart failure: Role of impaired

529 Ca^{2+} signaling and cytoskeletal reorganization. *Circulation Research*. **106** (6), 1103-1116 (2010).
530 26. Goncalves-Rodrigues, P., Miranda-Silva, D., Leite-Moreira, A. F., Falcao-Pires, I. Studying
531 left ventricular reverse remodeling by aortic debanding in rodents. *Journal of Visualized*
532 *Experiments*. **173**, e60036 (2021).
533 27. Miranda-Silva, D. et al. Characterization of biventricular alterations in myocardial
534 (reverse) remodelling in aortic banding-induced chronic pressure overload. *Scientific Reports*. **9**,
535 2956 (2019).
536 28. Chou, S. H. et al. The effects of debanding on the lung expression of ET-1, eNOS, and cGMP
537 in rats with left ventricular pressure overload. *Experimental Biology and Medicine (Maywood)*.
538 **231** (6), 954-959 (2006).
539 29. Hentschel, T. et al. Inhalation of the phosphodiesterase-3 inhibitor milrinone attenuates
540 pulmonary hypertension in a rat model of congestive heart failure. *Anesthesiology*. **106** (1), 124-
541 131 (2007).
542 30. Gs, A. K., Raj, B., Santhosh, K. S., Sanjay, G., Kartha, C. C. Ascending aortic constriction in
543 rats for creation of pressure overload cardiac hypertrophy model. *Journal of Visualized*
544 *Experiments*. **88**, e50983 (2014).
545 31. Angermann, C. E., Ertl, G. Natriuretic peptides--new diagnostic markers in heart disease.
546 *Herz*. **29** (6), 609-617 (2004).
547 32. Ordodi, V. L., Paunescu, V., Mic, F. A. Optimal access to the rat heart by transverse
548 bilateral thoracotomy with double ligature of the internal thoracic arteries. *American Association*
549 *for Laboratory Animal* Science. **47** (5), 44-46 (2008).
550 33. Fay, D. S., Gerow, K. A biologist's guide to statistical thinking and analysis. *WormBook*, 1-
551 54 (2013).
552 34. Etz, C. D. et al. Medically refractory pulmonary hypertension: treatment with nonpulsatile
553 left ventricular assist devices. *The Annals of Thoracic Surgery*. **83** (5), 1697-1705 (2007).
554 35. Mikus, E. et al. Reversibility of fixed pulmonary hypertension in left ventricular assist
555 device support recipients. *European Journal of Cardio-Thoracic Surgery*. **40** (4), 971-977 (2011).
556 36. Zelt, J. G. E., Chaudhary, K. R., Cadete, V. J., Mielniczuk, L. M., Stewart, D. J. Medical
557 therapy for heart failure associated with pulmonary hypertension. *Circulation Research*. **124** (11),
558 1551-1567 (2019).
559

Figure 1

Click here to access/download;Figure;Figure 1.psd

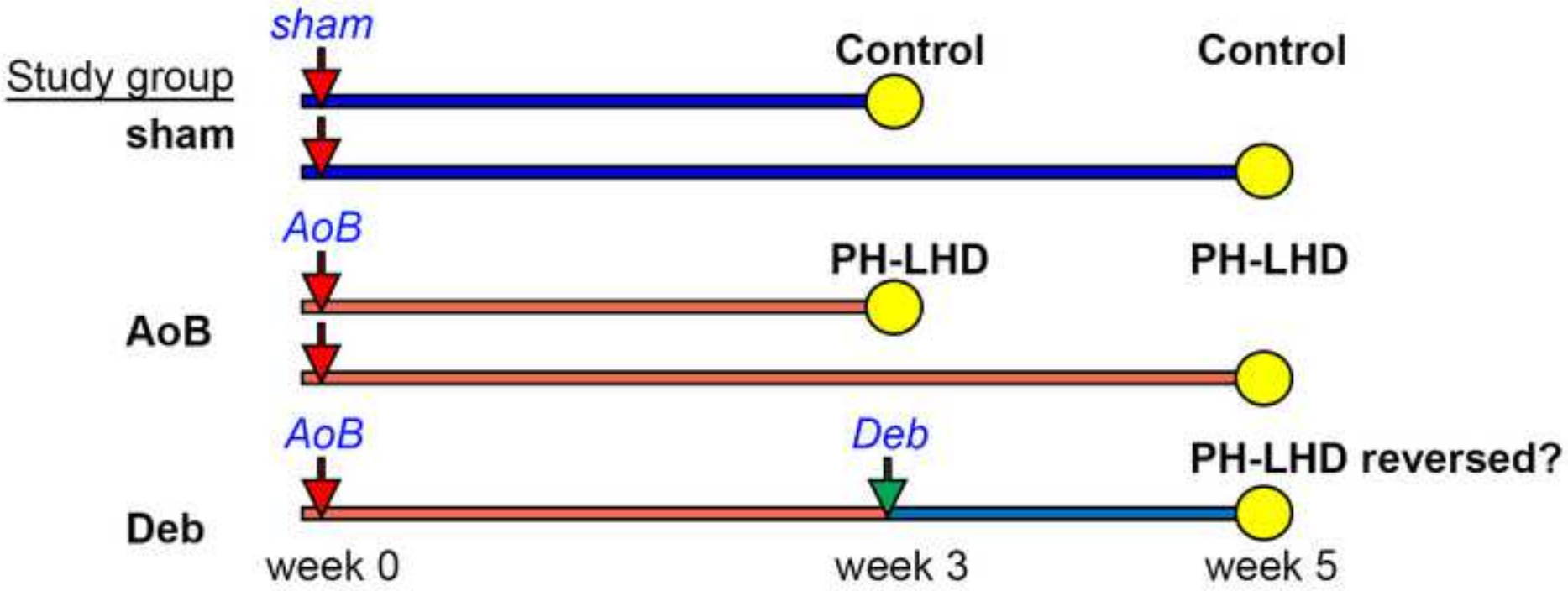

Figure 2

Click here to access/download;Figure;Figure 2.psd

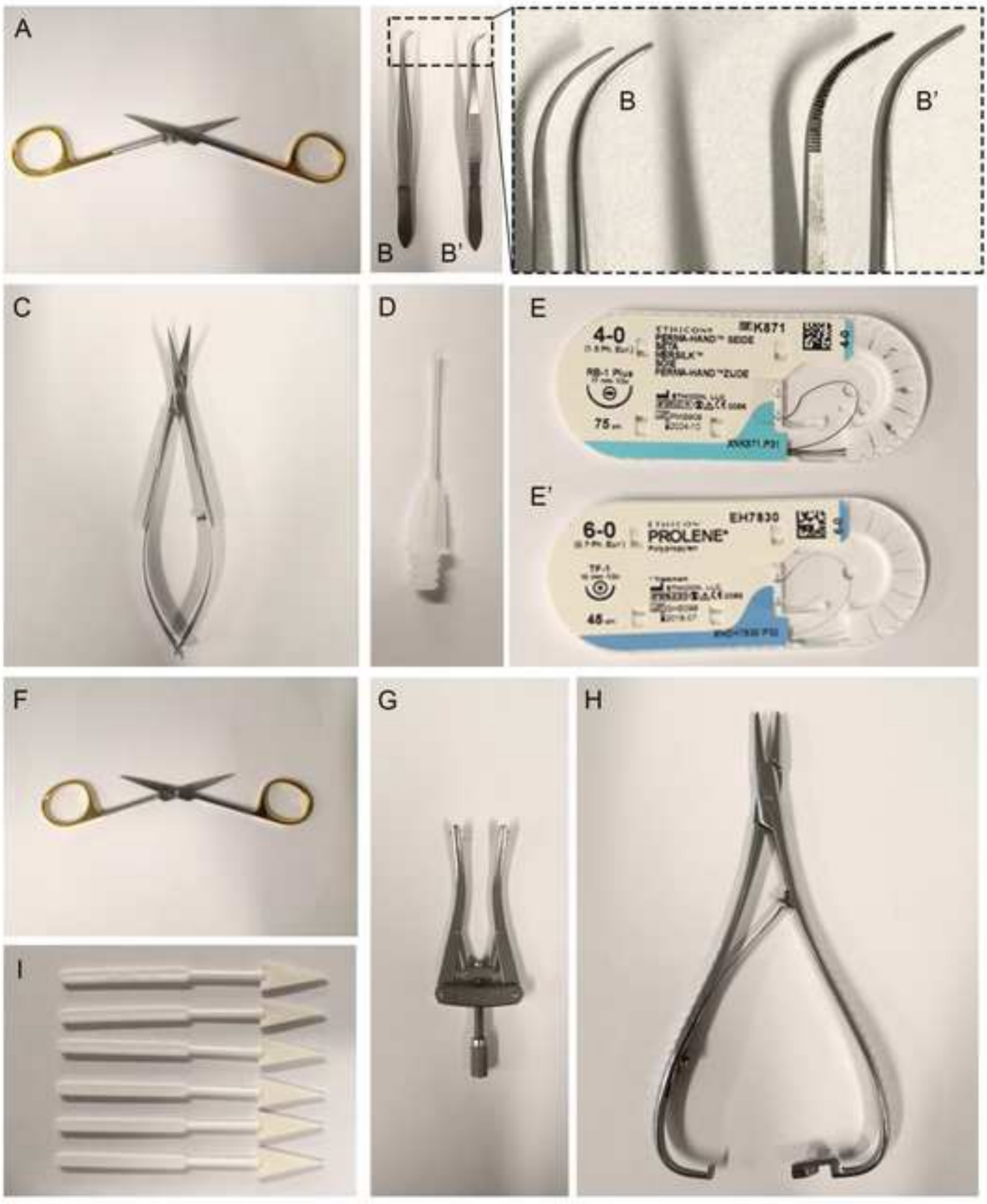

Figure 3

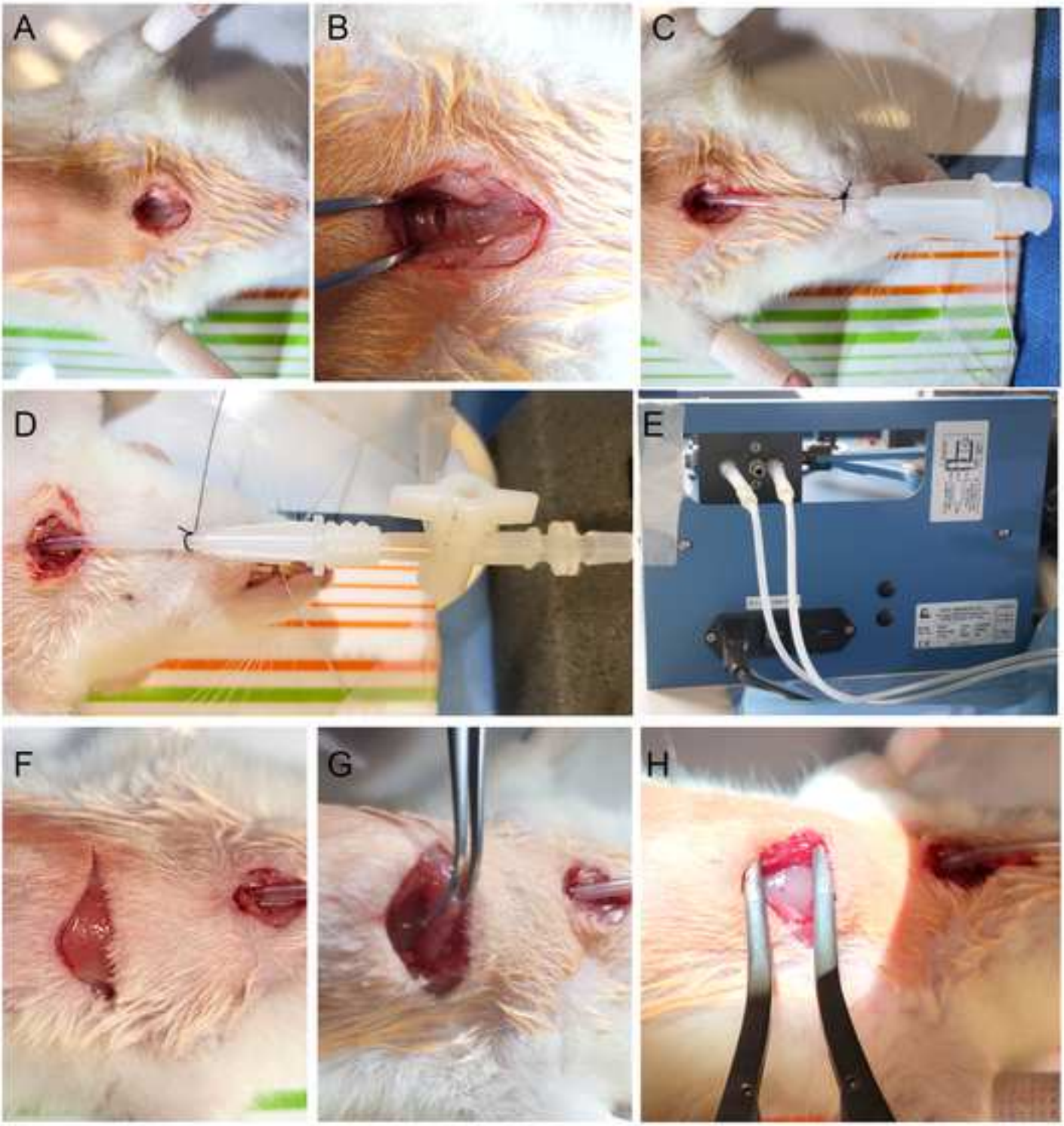

Figure 4

Click here to access/download;Figure;Figure 4.psd

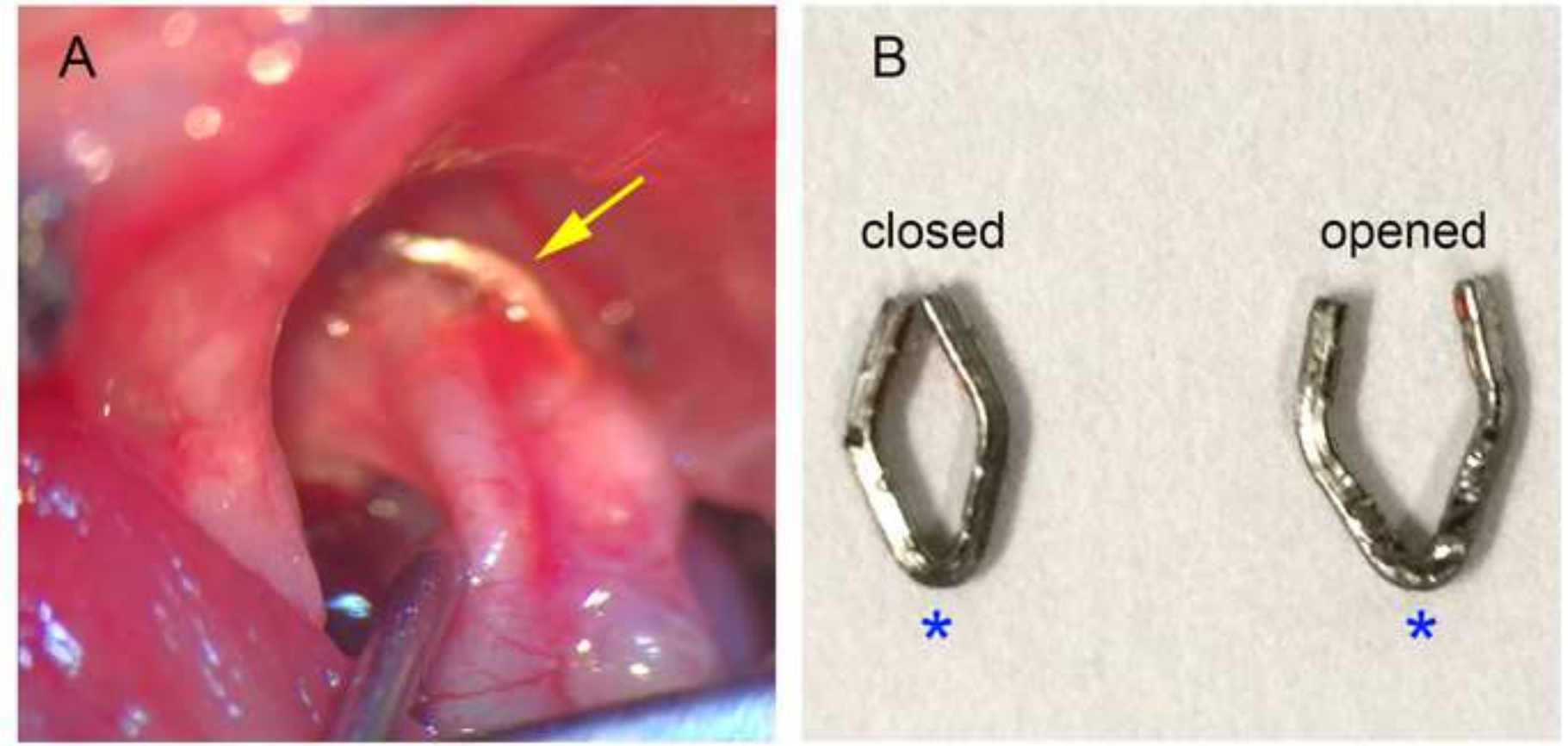

Figure 5

Click here to access/download;Figure;Figure 5.psd

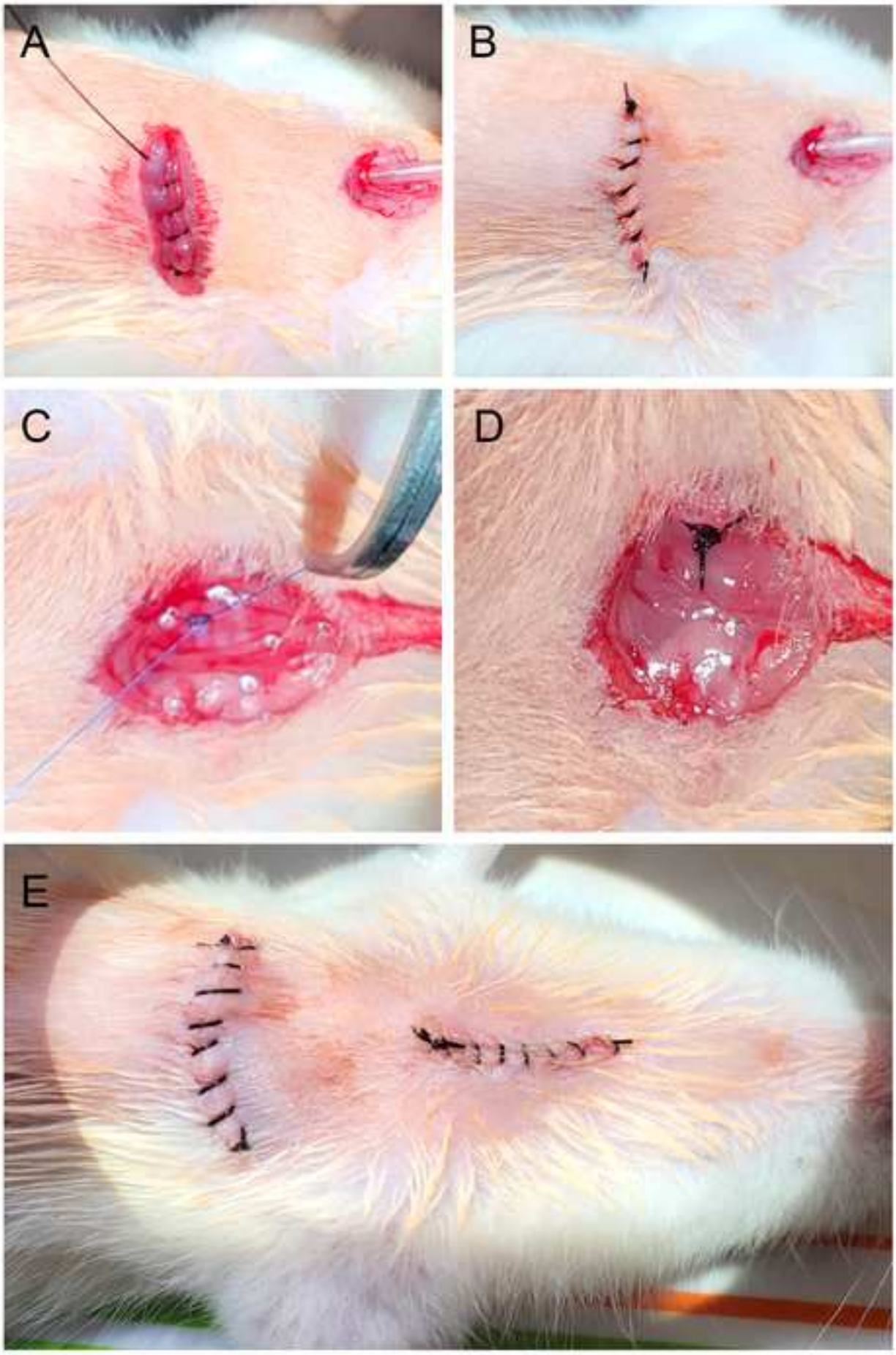

Figure 6

Click here to access/download;Figure;Figure 6.psd

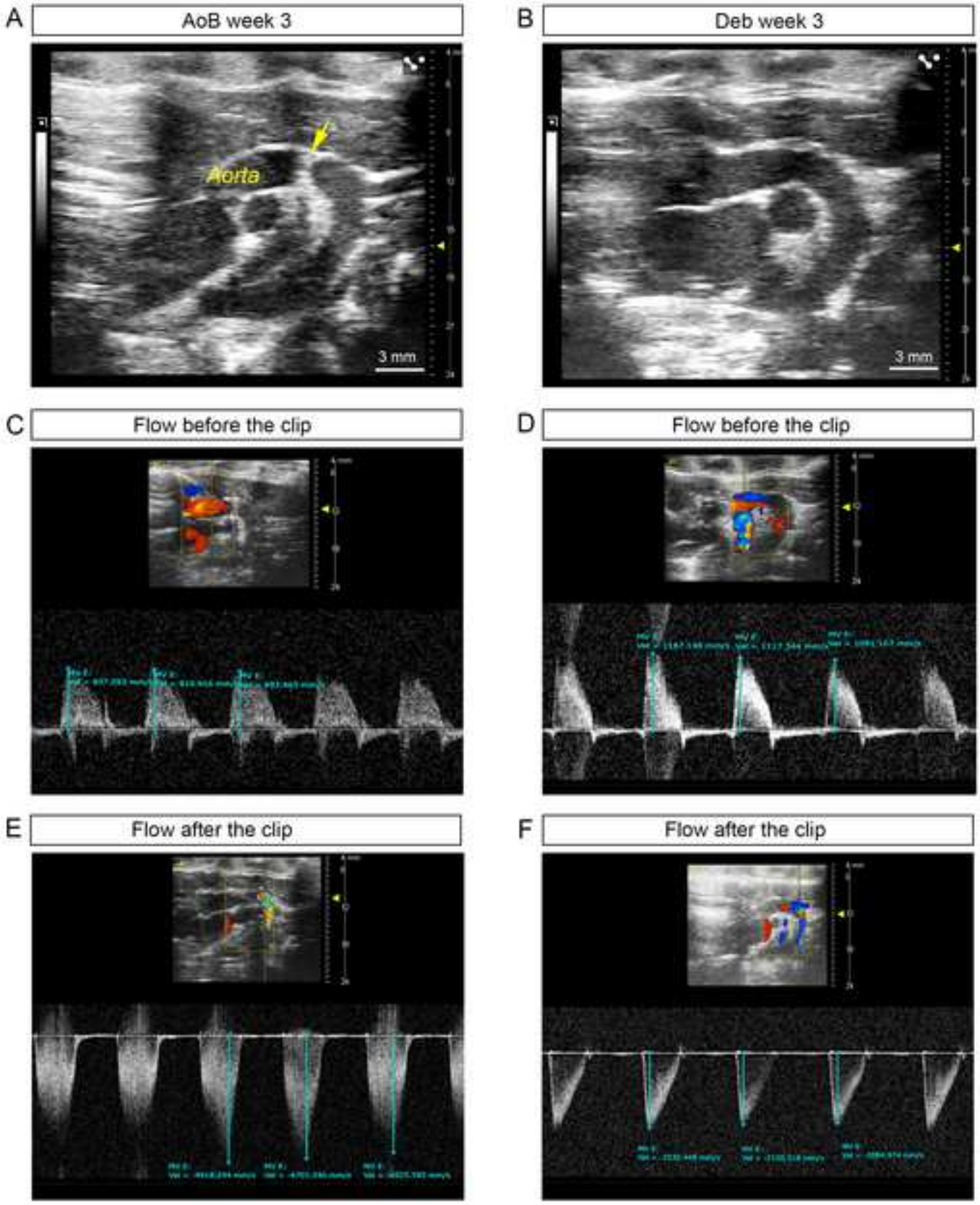

Figure 7

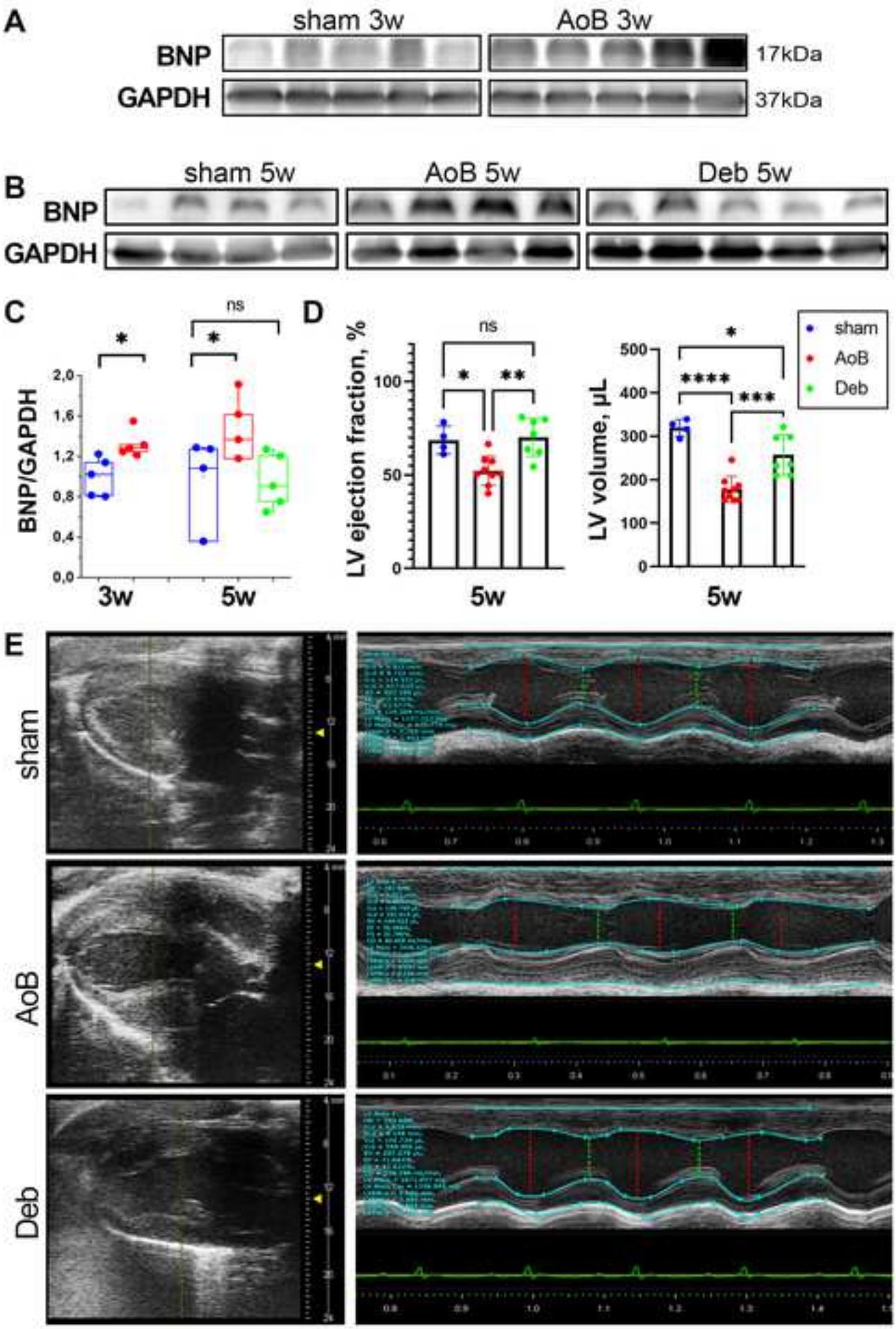

Figure 8

Click here to access/download;Figure;Figure 8.psd

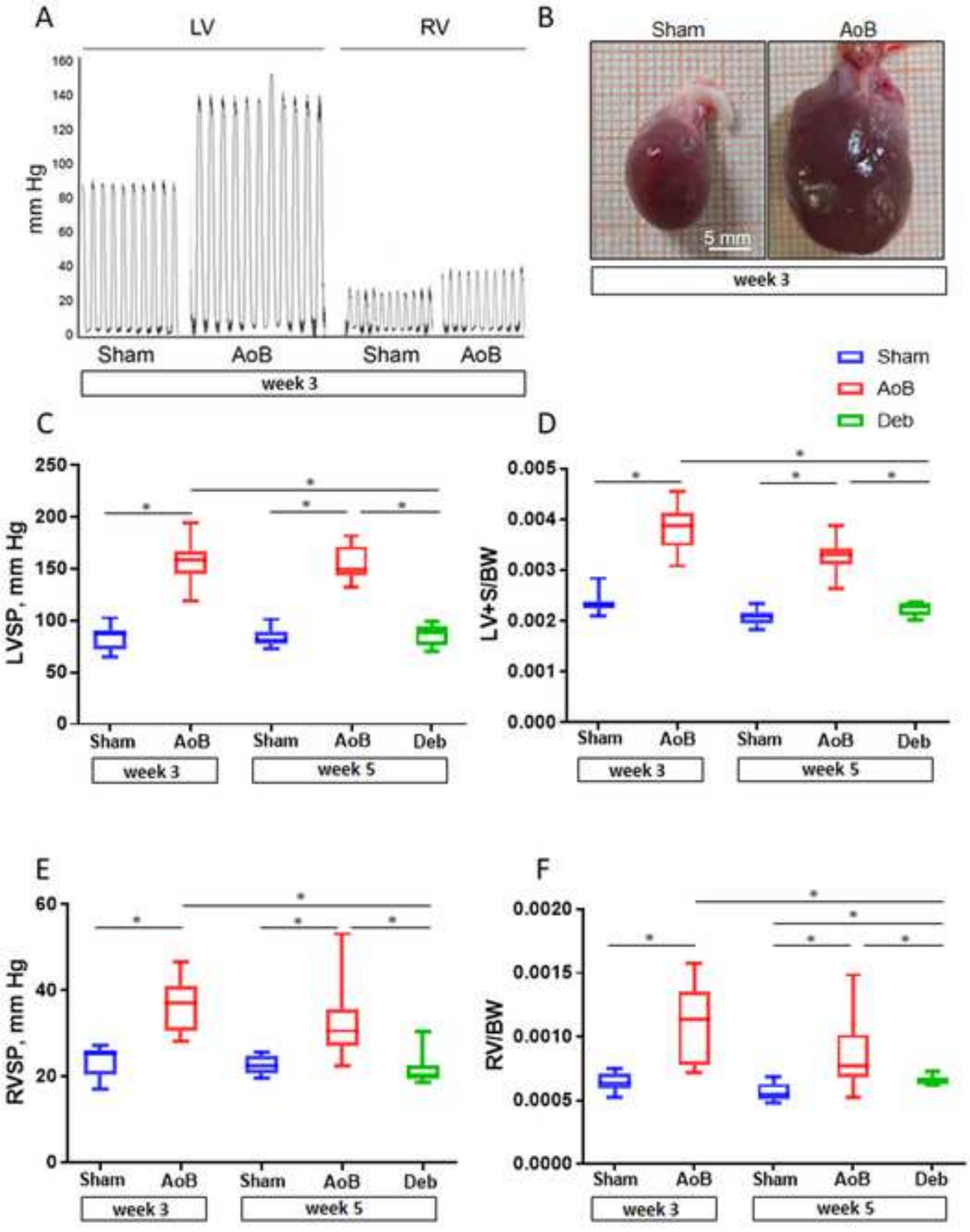

Manoj Kumar Jana, Ph.D.
Review Editor
JoVE
manoj.jana@jove.com

JoVE63502 "A model of reverse vascular remodeling in pulmonary hypertension due to left heart disease by aortic debanding in rats," by Pengchao Sang, Mariya M. Kucherenko, Juquan Yao, Qiuhua Li, Szandor Simmons, Wolfgang M. Kuebler, Christoph Knosalla

Dear Dr. Manoj,

We would like to thank the editor and reviewers for the careful evaluation of our manuscript and the helpful and pertinent comments. We have made changes to the manuscript as requested. Please find attached below a detailed point-by-point response to all comments. All modifications in the manuscript have been highlighted in red.

Sincerely,
Mariya Kucherenko, PhD
mariya.kucherenko@charite.de
[1]German Heart Center Berlin
Augustenburger Platz 1, 13353 Berlin;
[2]Institute of Physiology, Charité – Universitätsmedizin Berlin
Charitéplatz 1, 10117 Berlin

Response to the Editor:

1. Please take this opportunity to thoroughly proofread the manuscript to ensure that there are no spelling or grammar issues.
Done.

2. Please provide an email address for each author.
Email addresses for each author are provided in the manuscript.

3. Please revise the text to avoid the use of any personal pronouns (e.g., "we", "you", "our" etc.).
Done.

4. For in-text formatting, corresponding reference numbers should appear as numbered superscripts without brackets after the appropriate statement(s), but before the punctuation.
References are reformatted.

5. JoVE cannot publish manuscripts containing commercial language. This includes trademark symbols (™), registered symbols (®), catalog numbers, and company names before or after an instrument, reagent, or tool. Please remove all commercial language from your manuscript and use generic terms instead. All commercial products should be sufficiently referenced in the Table of Materials (For example: Janvier labs, Vevo®, Vevo LAB, FUJIFILM VisualSonics, Millar, PowerLab, ADInstruments, F.S.T item No.14568-12, Ethicon, EH7830, AE-BV010R, Sugi Saugtupfer tissue, REF 30601).
All commercial language has been removed from the text, and the Supplementary table was adjusted accordingly.

6. Please ensure that the Introduction also includes the following:
a) The advantages over alternative techniques with applicable references to previous studies
b) A description of the context of the technique in the wider body of literature
c) Information to help readers to determine whether the method is appropriate for their application
In response to this comment, the Introduction has been rewritten to include these points (pages 3-4). The revised passages now read as follows:
Page 3, Lines 93-101: "In comparison to similar heart failure due to pressure overload in the murine model of transverse aortic constriction (TAC) [17], banding of the ascending aorta above the aortic root in AoB rats does not produce hypertension in the left carotid artery as the banding site is proximal of the outflow of the left carotid artery from the aorta. As a result, AoB does not cause left-sided neuronal injury in the cortex as is characteristic for TAC [18], and which may affect study outcome. As compared to other rodent models of surgically induced PH-LHD, rat models in general and AoB in particular prove to be more robust, reproducible, and replicate the remodeling of the pulmonary circulation characteristic for PH-LHD patients, while perioperative lethality is low (reviewed in [19])."

Pages 3-4, Lines 113-126: "Moreover, a limited number of earlier studies have explored the effects of aortic debanding on PH-LHD in rats and showed that aortic debanding may reverse medial hypertrophy in pulmonary arterioles, normalize the expression of pre-pro-endothelin 1 and improve pulmonary hemodynamics [27,28], providing evidence for the reversibility of PH in rats with heart failure. Here, we optimized and standardized the technical procedures of the debanding surgery, e.g. by applying a

tracheotomy instead of endotracheal intubation, or by using titanium clips of a defined inner diameter for aortic banding instead of polypropylene sutures with a blunt needle (as reported in [26,27]), thus providing for better control of the surgical procedures, increased reproducibility of the model and an improved survival rate.

From a scientific perspective, the significance of the PH-LHD debanding model does not solely lie on demonstrating the reversibility of the cardio-vascular and pulmonary phenotype in heart failure, but more importantly in the idenfitication of molecular drivers that trigger and/or sustain reverse remodeling in pulmonary arteries as promising candidates for future therapeutic targeting."

7. Please consider including more figures (besides Figure 3A) to illustrate the surgical steps as the Protocol mainly involves surgery.

Two new figures (new Figure 3 and 5) have been incorporated to better illustrate surgical procedures. References to these and the other figures in the text are readjusted accordingly. New figure legends are added (please also see below).

8. Step 5.1: Please mention if the animal is kept alone in the cage during recovery.

This has been clarified as follows:

Page 6, Line 234: "Only keep one animal per recovery cage at any time".

9. Lines 238-239: The details of median thoracotomy, cardiac catheterization and euthanasia are not given in the present Protocol. Please provide the experimental details or refer to previously published protocol, if any.

In response to this comment, we have included a reference to a published protocol for the thoracotomy, and included additional details on cardiac catheterization and euthanasia into the text as follows:

Page 7, Lines 268-273: "In brief, rats were again anesthetized with ketamine (87 mg/kg bw) and xylazine (13 mg/kg bw), tracheotomized and ventilated as described above. Cardiac catheterization was performed after median thoracotomy [32] through the apex of (first) the left and (second) the right ventricle, respectively, as direct catheterization of the left ventricle via the vascular route is prevented by the aortic band in AoB animals. Following euthanasia by an overdose of ketamine/xylazine, …"

10. Figure 4C-F: The labels "flow before/after the clip" are not discussed in the legend. Please discuss. Also, mention the time point of analyses in the legend.

Changes in figure legend are introduced as follows:

Page 8, Lines 319-324: "Pulsed-wave Doppler echocardiographic images show blood flow before the clip in an AoB rat (C) and blood flow in the corresponding aortic segment in a Deb rat (D) taken one day prior and one day after the aortic debanding surgery, respectively. E-F, Analogously, images show blood flow in the aortic segment after the clip in an AoB rat (E) and in the corresponding aortic segment in a Deb rat (F) taken one day prior and one day after the aortic debanding surgery, respectively".

11. Figure 5B: Please include a scale bar

Done.

12. Figure 5C-F: Please specify with respect to what are the parameters in deb group normalized? Also, please define the error bars.

Done.

Page 9, Lines 348-349: "(in comparison to 3- and 5-week AoB groups) in Deb rats. Boxes show median, 25 and 75 percentiles, respectively; whiskers indicate minimum and maximum values."

13. As we are a methods journal, please revise the Discussion to explicitly cover the following in detail in 3-6 paragraphs with citations:
a) Critical steps within the protocol
b) Any modifications and troubleshooting of the technique
c) Any limitations of the technique
d) The significance with respect to existing methods
e) Any future applications of the technique

In response to this comment, the Discussion has been rewritten to include these points. The revised passages now read as follows:

Pages 10-11, Lines 384-424: "The success of the technically challenging aortic debanding procedure in AoB rats depends not only on surgical skills but also on precise perioperative procedures. Outlined in the following are critical steps of the surgical procedure that may cause perioperative lethality by either excessive bleeding (critical steps 1-5) or insufficient respiration (critical step 6) and recommendations on how to avoid these complications:

1. During thoracotomy the midsternal line should be approached carefully with the scissors to avoid injury to the internal mammary artery.
2. In order to visualize the heart and the conduit arteries, the thymus should be mobilized and carefully relocated in cranial direction. In the debanding surgery, the thymus tissue is often found connected to the heart and arteries via post-operative adhesions from the original AoB surgery. These adhesions should be carefully separated with a pair of blunt forceps to avoid injury of the cardiovascular structures.
3. In the debanding surgery, the aorta with the clip is frequently embedded in connective tissue. To visualize the clip, this connective tissue must be gently dissected with a blunt forceps. Here, the transthoracic echocardiography performed prior to the surgery is a helpful preparation step, allowing to identify in advance whether the clip is located close to the aortic root, in the middle of the ascending aorta, or close to the brachiocephalic artery. This knowledge saves precious time for clip allocation during the surgery.
4. The orientation of the clip is a critical step that must be considered carefully during the initial aortic banding surgery. To facilitate optimal assessment and rapid opening of the clip during aortic debanding, the part of the clip that needs to be compressed by the needle holder (Figure 4B) should be oriented ventrally. Clip reorientation during debanding surgery is feasible, although at the risk of injury to the aorta. For clip reorientation, clips should be held by a forceps while surrounding connective tissue is carefully removed, then the clip should be mobilized and turned. Holding the aorta with the forceps is to be avoided.
5. For debanding the clip should be held by a forceps with one hand and opened with a needle holder by the other hand. The aorta should not be lifted ventrally.
6. After successful completion of the debanding procedure, extubated PH-LHD rats are at considerable risk of respiratory failure, with animals commonly dying within 10-20 min after surgery while still under the anesthesia. Atelectasis of the left lung is the most common cause of death in this period, and prolonged mechanical ventilation prior to chest closure helps to recruit the lung and to warrant sufficient respiration after surgery.

The present study reports an aortic debanding technique performed 3 weeks after initial aortic banding in rats. For studies aiming to compare reverse remodeling of the pulmonary vasculature and the RV at different stages of PH, the described procedures may also be performed at later time points after aortic banding, yet caution is warranted as scar and connective tissue surrounding the aorta is likely to become more abundant with time, further complicating the procedure and necessitating additional troubleshooting and refinement, while the basic principles of the reported protocol still apply."

14. Please ensure that the references appear as the following: [Lastname, F.I., LastName, F.I., LastName, F.I. Article Title. Source. Volume (Issue), FirstPage – LastPage (YEAR).] For more than 5 authors, list only the first author then et al. Please expand journal names.
Done.

Response to Reviewer 1:

Manuscript Summary:
In this manuscript, the authors report a surgical procedure to remove ascending-aortic constriction in rat model of pulmonary hypertension due to left heart diseases by aortic banding. This technique allows
studying endogenous mechanisms of reverse remodeling in the pulmonary circulation and the right heart, informing strategies to reverse pulmonary hypertension and/or right ventricular dysfunction.

Major Concerns:
No major concerns. The methods are clearly explained and well organized. Readers should be able to follow the protocol and reproduce the results presented in the discussion.
We thank the reviewer for the positive evaluation of our manuscript and the encouraging comments.

Minor Concerns:
Introduction can be simplified and focused on how this model compares to other available models of PH-LHD.
We thank the reviewer for this constructive comment. In response, we have revised the introduction to discuss the current model in the context of other models of heart failure and debanding, respectively. The revised passages now read as follows:

Page 3, Lines 93-101: "In comparison to similar heart failure due to pressure overload in the murine model of transverse aortic constriction (TAC) [17], banding of the ascending aorta above the aortic root in AoB rats does not produce hypertension in the left carotid artery as the banding site is proximal of the outflow of the left carotid artery from the aorta. As a result, AoB does not cause left-sided neuronal injury in the cortex as is characteristic for TAC [18], and which may affect study outcome. As compared to other rodent models of surgically induced PH-LHD, rat models in general and AoB in particular prove to be more robust, reproducible, and replicate the remodeling of the pulmonary circulation characteristic for PH-LHD patients, while perioperative lethality is low (reviewed in [19])."

Pages 3-4, Lines 113-126: "Moreover, a limited number of earlier studies have explored the effects of aortic debanding on PH-LHD in rats and showed that aortic debanding may reverse medial hypertrophy in pulmonary arterioles, normalize the expression of pre-pro-endothelin 1 and improve pulmonary hemodynamics [27,28], providing evidence for the reversibility of PH in rats with heart failure. Here, we optimized and standardized the technical procedures of the debanding surgery, e.g. by applying a tracheotomy instead of endotracheal intubation, or by using titanium clips of a defined inner diameter for aortic banding instead of polypropylene sutures with a blunt needle (as reported in [26,27]), thus providing for better control of the surgical procedures, increased reproducibility of the model and an improved survival rate.

From a scientific perspective, the significance of the PH-LHD debanding model does not solely lie on demonstrating the reversibility of the cardio-vascular and pulmonary phenotype in heart failure, but more importantly in the idenfitication of molecular drivers that trigger and/or sustain reverse remodeling in pulmonary arteries as promising candidates for future therapeutic targeting."

Response to Reviewer 2:

I. Manuscript Summary:

Firstly, I do thank you for giving me the important chance to read the interesting article, in which the debanding was well written. In fact, that there were already some articles in which various debanding procedures were reported in rat models with pulmonary hypertension secondary to left heart failure by banding aorta. For example, it has been reported earlier that debanding could result in both reversal of PH and attenuation of the expression of ET-1 in the aortic banded group (Exp Biol Med (Maywood). 2006 Jun;231(6):954-9).

We thank the reviewer for the positive evaluation of our manuscript and the reference to the 2006 paper by Chou and coworkers, which has now been included into the revised manuscript as reference **28** Chou, S. H. et al. The effects of debanding on the lung expression of ET-1, eNOS, and cGMP in rats with left ventricular pressure overload. Exp Biol Med (Maywood) 231, 954-959 (2006).

II. Major concerns:

I have some suggestions as follow;

1) I just wonder whether there could be different hemodynamic effects of banding between 1 cm above aortic root and transvere aorta.

We thank the reviewer for raising this relevant question. In the revised manuscript, we have added new text to address this point as follows:

Page 3, Lines 93-98: "In comparison to similar heart failure due to pressure overload in the murine model of transverse aortic constriction (TAC) [17], banding of the ascending aorta above the aortic root in AoB rats does not produce hypertension in the left carotid artery as the banding site is proximal of the outflow of the left carotid artery from the aorta. As a result, AoB does not cause left-sided neuronal injury in the cortex as is characteristic for TAC [18], and which may affect study outcome."

2) I would suggest to do directly endotracheal intubation instead of tracheostomy while debanding.

We thank the reviewer for this suggestion. Indeed, previous studies on aortic debanding performed direct endotracheal intubation instead of tracheostomy during the debanding surgery (References **26**,**27**). We suggest, however, that in comparison to endotracheal intubation tracheostomy provides for better control of appropriate ventilation during the surgical procedures, which is specifically relevant during aortic debanding. This notion is based on the following rationale:

- Tracheostomy, which is routinely perform in our lab for perioperative lung ventilation, is a straightforward and safe technique with no perioperative or postoperative complications.
- Tracheostomy eliminates the risk of esophageal intubation or tracheal injury; it enables precise positioning and fixation of the tracheal cannula and constant visual control of the cannula during all steps of the surgical procedure.
- At the time of aortic debanding, AoB animals are already in heart failure and as such more sensitive to additional stress; as a result the potential risks that come with endotracheal intubation may add to increased lethality.
- Finally, when the operated animal is weaned from the ventilator but fails to develop spontaneous breathing, a tracheostomy allows for rapid reintubation and reconnection with the ventilator, thus potentially saving lives due to the ability for prolonged postoperative ventilation.

Based on these rationales, we would advocate for tracheostomy rather than endotracheal intubation for this specific and complex surgical intervention. As such, we have left the respective text passages referring to tracheostomy unchanged in the revised manuscript.

III. Minor concerns:

Please check the alterations of brain natriuretic peptide (BNP) in plasma and left ventricle for approving the improvement of left ventricular dysfunction.

We thank the reviewer for this insightful suggestion to verify the improvement of left ventricular function after debanding. We have gladly followed the reviewer´s advice and measured BNP expression in the left ventricle by Western blotting, which revealed an increase in BNP in AoB as compared to sham animals, which was, however, normalized by debanding. Unfortunately, we could not perform BNP measurements in corresponding plasma samples, as plasma had originally not been collected in our study. However, in addition to BNP data, we now provide additional data on left ventricular ejection fraction and volume as assessed by echocardiography in sham, AoB and Deb groups. These new results confirm the improvement of left ventricular function following debanding, and are now presented in new Figure 7 and the corresponding legend (New Figure and corresponding legends is below), and incorporated in the Results section as follows:

Page 7, Lines 256-265: "To probe for reversal of left heart failure by aortic debanding, we assessed the expression levels of brain natriuretic peptide (BNP), a clinical routine parameter for the assessment of heart disease[8], in the LV myocardium. At week 3 and 5 after aortic banding AoB animals showed a significantly increased production of BNP in comparison to sham operated controls, while Deb rats at week 5 expressed BNP at levels comparable to sham animals, indicating the reversal of LV failure by aortic debanding (Figure 7A-C). In parallel, evaluation of LV function by transthoracic echocardiography revealed an increased LV ejection fraction and LV volume in Deb animals as compared to AoB rats (Figure 7D-E). While LV ejection fraction in Deb animals was comparable to sham rats, LV volume in Deb rats failed to fully normalize to values seen in the sham group, indicating that reversal of LV function is incomplete."

New Figures:
Figure 3

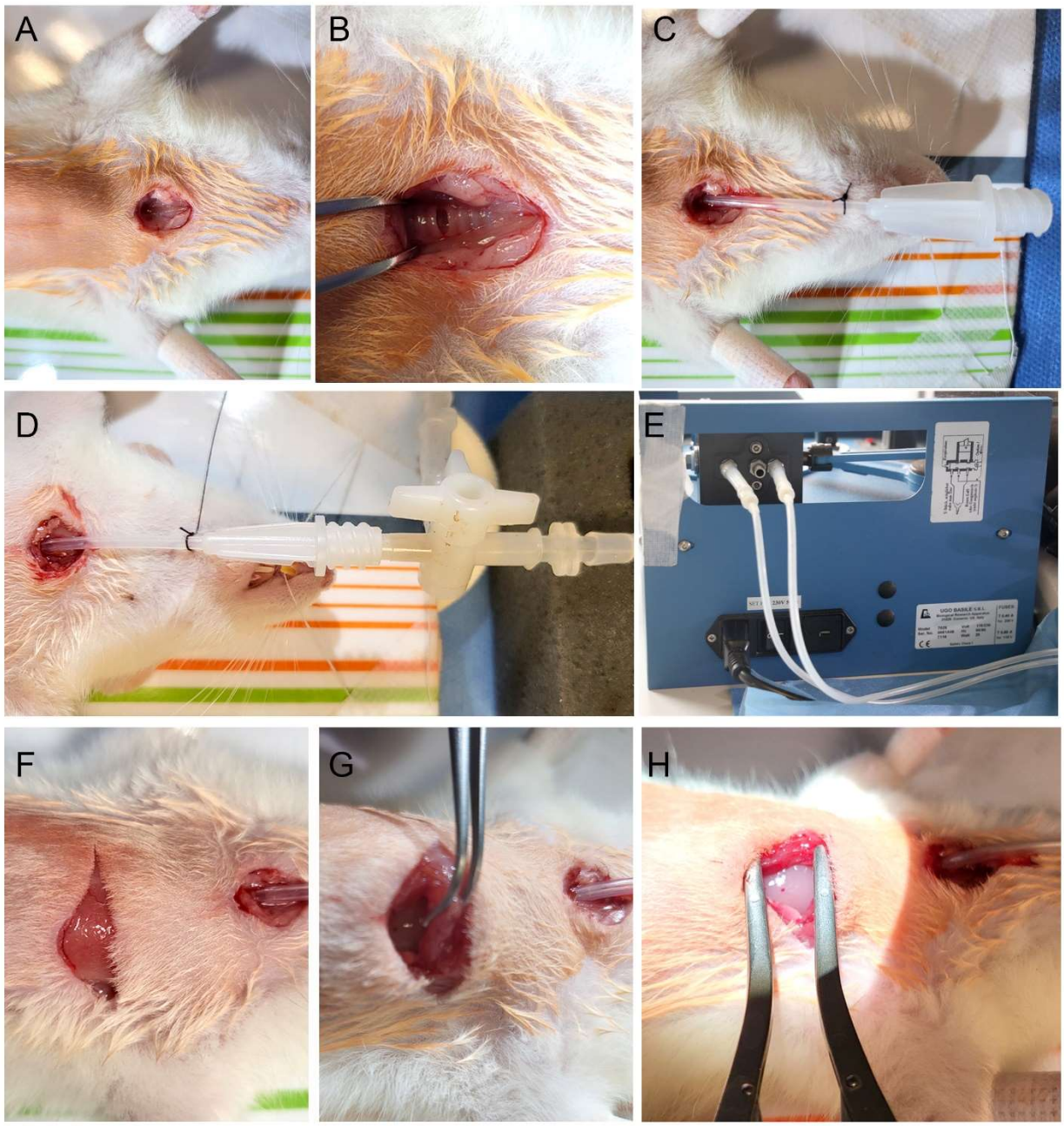

Figure 3. Tracheotomy and thoracotomy
Imagess illustrate the surgical steps for the tracheotomy: **A**, cervical midline incision; **B**, incision of the trachea between two cartilaginous rings; **C**, tracheal cannula inserted into the trachea and secured with a suture; **D**, tracheal cannula connected to a mechanical ventilator (shown in **E**). Images illustrate the surgical steps for the thoracotomy: **F**, skin incision between the second and third ribs; **G**, cutting of muscles; **H**, creation of a thoracic surgical window by spreading the second and the third ribs.

Figure 5

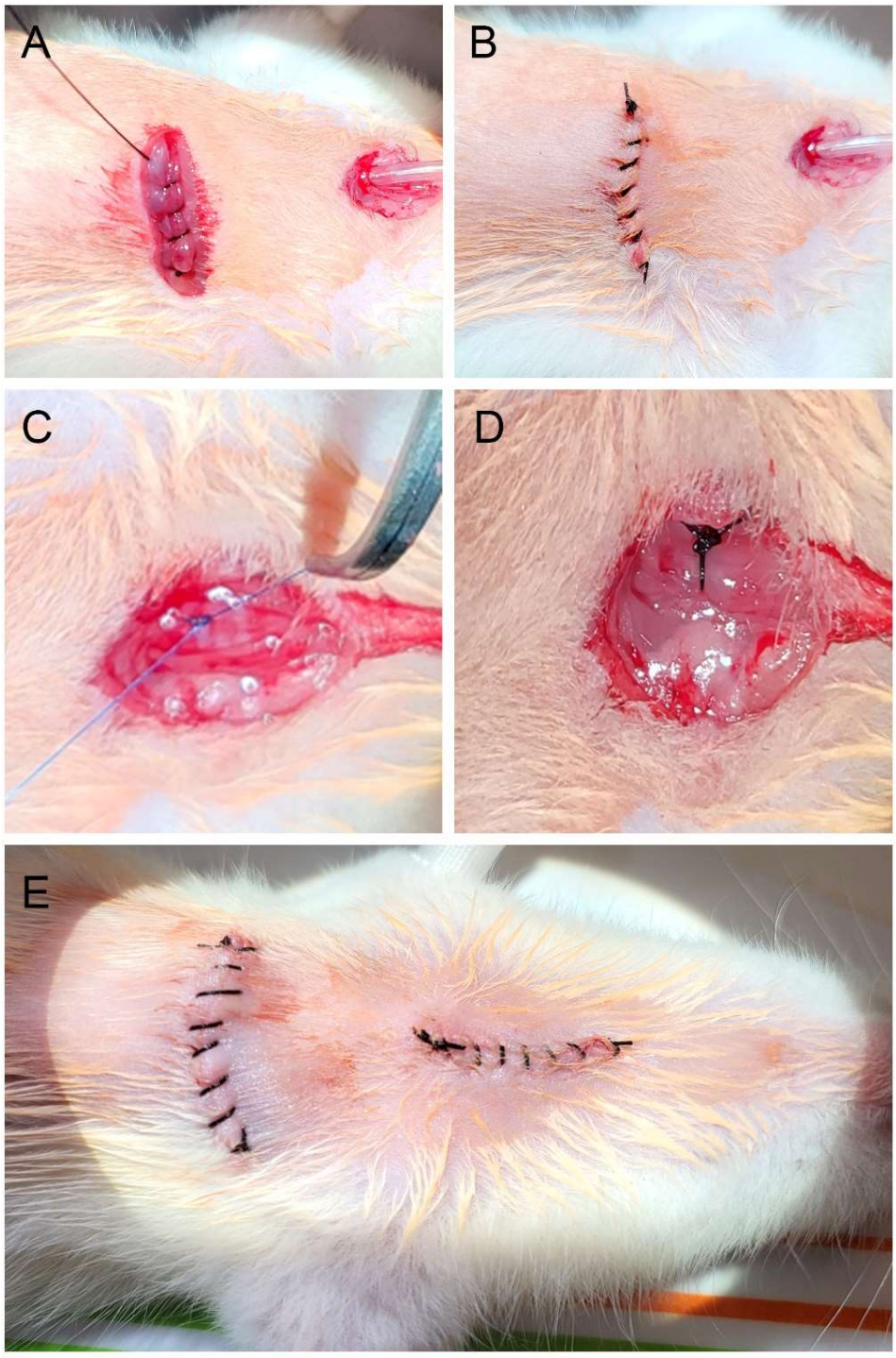

Figure 5. Wound closure
Images illustrate closing of the thoracic upper muscles (**A**) and the skin (**B**) with a simple continuous suture. The trachea (**C**) and the infrahyoid muscles (**D**) are closed by a simple suture and the skin on the neck (**D**) by a simple continuous suture.

Figure 7

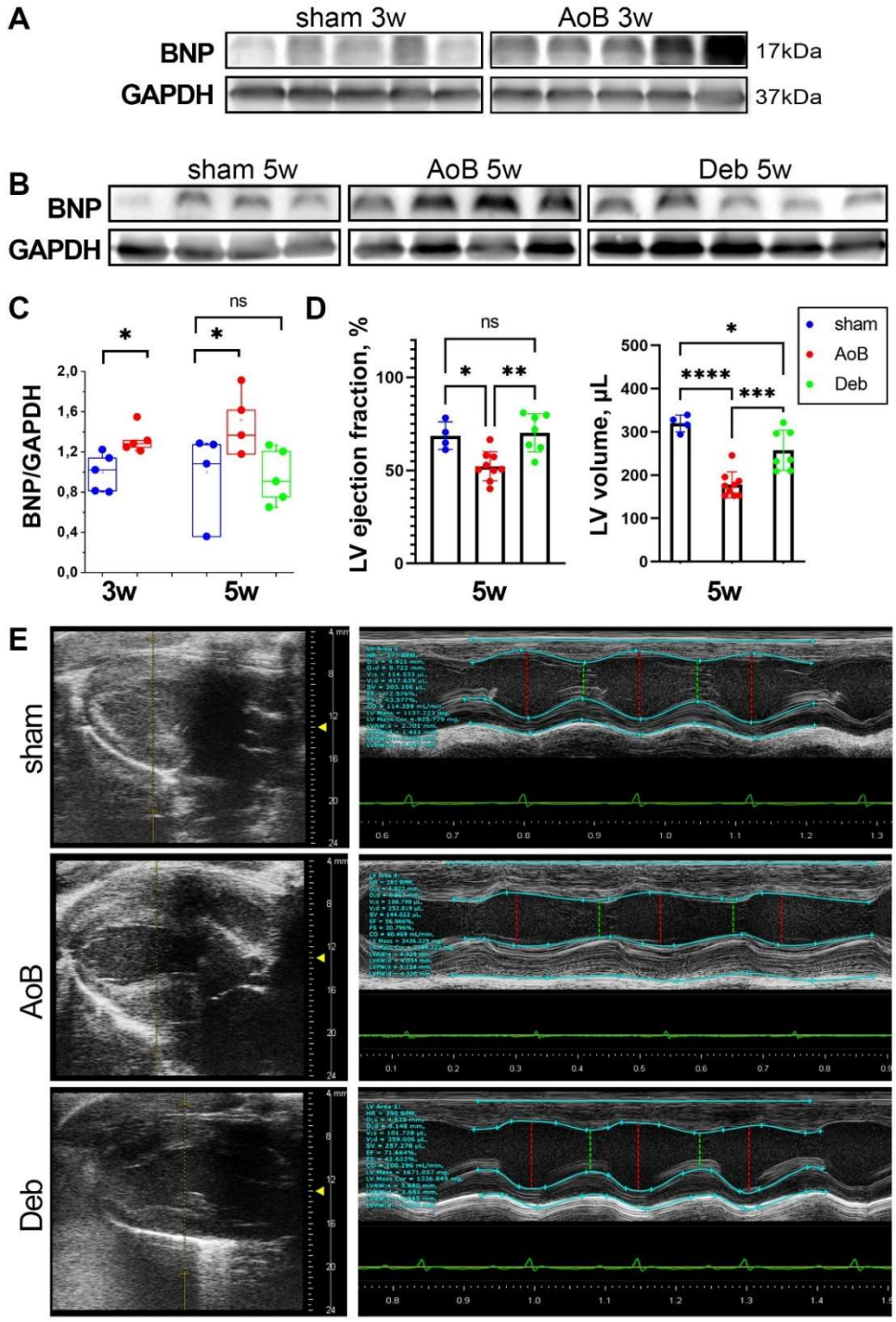

Figure 7. Normalization of left ventricular function by aortic debanding
A, Representative Western blots show protein levels of BNP and with GAPDH as loading control in left ventricles (LV) of AoB rats at week 3 after aortic banding (n=5) and in corresponding sham controls (n=5). **B**, Representative Western blots show BNP and GAPDH in left ventricles (LV) of AoB rats at week 5 after aortic banding (n=4), in Deb rats at week 5 (n=5),

and in sham controls at the corresponding time after primary surgery (n=4). **C**, Box and whisker plots show quantification of BNP expression normalized to GAPDH and sham control at the corresponding time after primary surgery. Boxes show median, 25 and 75 percentiles, respectively; whiskers indicate minimum and maximum values. For statistical analyses Student's t-test was used *, *p*-value < 0.05. **D**, Bar graphs (mean±standard deviation) show LV ejection fraction and volume in sham (n=4), AoB (n=9) and Deb (n=7) animals at week 5 as measured by echocardiography from M- and B-mode images. **E**, Representative M-mode echocardiographic images show changes in LV fractional shortening in sham, AoB and Deb animals at week 5. For statistical analyses Mann–Whitney U test was used *, *p*-value < 0.05.